

A White-Light-Emitting Molecule: Frustrated Energy Transfer between Constituent Emitting Centers

Sanghyuk Park,[†] Ji Eon Kwon,[†] Se Hun Kim,[†] Jangwon Seo,[†] Kyeongwoon Chung,[†] Sun-Young Park,[‡] Du-Jeon Jang,[‡] Begoña Milián Medina,[§] Johannes Gierschner,^{§,||} and Soo Young Park^{*,†}

Department of Materials Science and Engineering, Seoul National University, ENG 445, Seoul 151-744, Korea, Department of Chemistry, Seoul National University, NS60, Seoul 151-742, Korea, Institut de Ciència Molecular (ICMOL), University of Valencia, P.O. Box 22085, 46071 Valencia, Spain, and Madrid Institute for Advanced Studies, IMDEA Nanoscience, UAM, Modulo C-IX, AV. Tomás y Valiente 7, Campus de Cantoblanco, 28049 Madrid, Spain

Received March 31, 2009; E-mail: parksy@snu.ac.kr

Abstract: White-light-emitting single molecules are promising materials for use in a new generation of displays and light sources because they offer the possibility of simple fabrication with perfect color reproducibility and stability. To realize white-light emission at the molecular scale, thereby eliminating the detrimental concentration- or environment-dependent energy transfer problem in conventional fluorescent or phosphorescent systems, energy transfer between a larger band-gap donor and a smaller band-gap acceptor must be fundamentally blocked. Here, we present the first example of a concentration-independent ultimate white-light-emitting molecule based on excited-state intramolecular proton transfer materials. Our molecule is composed of covalently linked blue- and orange-light-emitting moieties between which energy transfer is entirely frustrated, leading to the production of reproducible, stable white photo- and electroluminescence.

Introduction

Synthesizing white-light-emitting single molecules is currently an exciting challenge in synthetic chemistry because of the possibility of innovative applications to new classes of displays^{1–3} and light sources.^{4,5} Compared to the multicomponent molecular emitters of white-light-emitting organic light-emitting devices (WOLEDs), use of a single molecule would enable easy fabrication with perfect color reproducibility and stability.^{6–8} All of the white-light-emitting molecules reported to date, without exception, are composed of covalently linked emitter components and utilize partial energy transfer from a wide band-gap donor component to a smaller band-gap acceptor to generate

white light covering the visible range from 400 to 700 nm. For instance, Coppo and colleagues reported white-light emission from a single molecule in solution; the molecule was composed of luminescent iridium and europium complexes, and partial energy transfer was involved.⁹ Yang and co-workers synthesized a pH-dependent organic white-light-emitting fluorophore composed of benzo[*a*]- and [b]xanthene derivatives.¹⁰ Because energy transfer characteristics in conventional fluorescent or phosphorescent systems depend strongly on donor–acceptor distance and mutual orientation, and thus on the concentrations and/or morphologies of these materials in the final device, the reported systems showed white-light emission only under very specific conditions. Therefore, the synthesis of efficient and color-stable white-light-emitting single molecules, not affected by the environment, is exceedingly difficult using the strategies reported to date.

To achieve white-light emission on a molecular scale, without concentration-dependent energy transfer problems, energy transfer between donor and acceptor must be fundamentally blocked. To date, various concepts, based on an unpopulated ground state of the energy acceptor, have been proposed; these include use of an excimer,⁸ the exciplex approach,¹¹ interligand energy

[†] Department of Materials Science and Engineering, Seoul National University.

[‡] Department of Chemistry, Seoul National University.

[§] University of Valencia.

^{||} Madrid Institute for Advanced Studies.

- (1) Andersson, P.; Nilsson, D.; Svensson, P. O.; Chen, M. X.; Malmstrom, A.; Remonen, T.; Kugler, T.; Berggren, M. *Adv. Mater.* **2002**, *14*, 1460.
- (2) Kido, J.; Kimura, M.; Nagai, K. *Science* **1995**, *267*, 1332.
- (3) Chen, Y.; Au, J.; Kazlas, P.; Ritenour, A.; Gates, H.; McCreary, M. *Nature* **2003**, *423*, 136.
- (4) Hayes, R. A.; Feenstra, B. J. *Nature* **2003**, *425*, 383.
- (5) Sun, Y. R.; Giebink, N. C.; Kanno, H.; Ma, B. W.; Thompson, M. E.; Forrest, S. R. *Nature* **2006**, *440*, 908.
- (6) Segal, M.; Singh, M.; Rivoire, K.; Difley, S.; Van Voorhis, T.; Baldo, M. A. *Nat. Mater.* **2007**, *6*, 374.
- (7) Mazzeo, M.; Vitale, V.; Della Sala, F.; Anni, M.; Barbarella, G.; Favaretto, L.; Sotgiu, G.; Cingolani, R.; Gigli, G. *Adv. Mater.* **2005**, *17*, 34.
- (8) Liu, Y.; Nishiura, M.; Wang, Y.; Hou, Z. M. *J. Am. Chem. Soc.* **2006**, *128*, 5592.

(9) Coppo, P.; Duati, M.; Kozhevnikov, V. N.; Hofstraat, J. W.; De Cola, L. *Angew. Chem., Int. Ed.* **2005**, *44*, 1806.

(10) Yang, Y. J.; Lowry, M.; Schowalter, C. M.; Fakayode, S. O.; Escobedo, J. O.; Xu, X. Y.; Zhang, H. T.; Jensen, T. J.; Fronczek, F. R.; Warner, I. M.; Strongin, R. M. *J. Am. Chem. Soc.* **2006**, *128*, 14081.

(11) Mazzeo, M.; Pisignano, D.; Della Sala, F.; Thompson, J.; Blyth, R. I. R.; Gigli, G.; Cingolani, R.; Sotgiu, G.; Barbarella, G. *Appl. Phys. Lett.* **2003**, *82*, 334.

transfer (ILET),¹² and excited-state intramolecular proton transfer (ESIPT) systems.¹³ However, these “frustrated energy transfer” strategies for constructing a white-emitting molecular dyad have yet to be demonstrated, although few cases of white-emitting molecule based on “partial energy transfer” have been reported.¹⁴ As a promising step toward our goal of designing white-light-emitting molecules devoid of the energy transfer problem, we exploited a pair of hydroxy-substituted tetraphenyl imidazole derivatives as complementary and independent emissive components based on frustration of energy transfer between these materials. This arises because of ESIPT, as previously demonstrated with a molecular mixture,¹³ leading to an energy state mismatch arising from the lack of a ground-state population in the acceptor.¹⁵

Here, we report the first example of a concentration-independent ultimate white-light-emitting molecular dyad based on two ESIPT keto-emitting units. These molecules are covalently linked blue- and orange-light-emitting moieties between which energy transfer is frustrated, and the combination thus shows broad white photoluminescence covering the entire visible range after single-wavelength excitation, as well as stable white electroluminescence, upon simple OLED device fabrication.

Experimental Section

Measurements. Chemical structures were fully identified by ¹H NMR (JEOL, JNM-LA300), ¹³C NMR (Bruker, Avance DPX-300), MALDI-TOF mass spectrometry (Applied Biosystems Inc.; Voyager-DE STR Biospectrometry Workstation), GC–mass spectrometry (JEOL, JMS-AX505WA), and elemental analysis (CE Instruments, EA1110). Absorption spectra were obtained using either of two UV–vis spectrophotometers (Scinco S-2040 and Shimadzu UV-1650PC). Photoluminescence emission and excitation spectra were obtained using a fluorescence spectrophotometer (Varian, Cary Eclipse); excitation spectra were corrected for characteristics of the light source. Emission spectra were corrected for wavelength-dependent sensitivity of the detector. Photoluminescence quantum efficiencies (Φ_{PL} values) for solutions were obtained using 9,10-diphenylanthracene as reference.¹⁶ The Φ_{PL} values of thin films on quartz plates were measured using a 6 in. integrating sphere (Labsphere, 3P-GPS-060-SF) equipped with a 325 nm CW He–Cd laser (Omnichrome, Series 56) and a PMT detector (Hamamatsu, PD471) attached to a monochromator (Acton Research, Spectrapro-300i). The detailed procedure followed to obtain solid-state Φ_{PL} data has been described elsewhere.¹⁷ Pulse-excited emission spectra were measured using an actively/passively mode-locked 25 ps Nd:YAG laser (Quantel, YG701) and an intensified CCD (Princeton Instruments, ICCD576G) attached to a spectrometer (Acton Research, Spectrapro-500) as the excitation source and detector, respectively. Samples were excited at the front face with pulses of 347 nm, generated through a Raman shifter filled with methane at 15 atm, and pumped by the fourth-harmonic pulses (266 nm) of the laser. A 10 ps streak camera (Hamamatsu, C2830) with a CCD detector (Princeton Instruments, RTE128H) was used for detection

of fluorescence kinetic profiles with excitation at the front face by 347 nm laser pulses. Emission wavelengths were selected by combining band-pass and cutoff filters. Fluorescence decay times were extracted by biexponential fitting procedures through deconvolution employing instrumental response functions. Differential scanning calorimetry (DSC) was carried out under a nitrogen atmosphere at a heating rate of 20 °C/min on a Perkin-Elmer DSC7. Cyclic voltammetric experiments were performed using a model 273A machine (Princeton Applied Research) with a one-compartment electrolysis cell consisting of a platinum working electrode, a platinum wire counter electrode, and a quasi Ag⁺/Ag electrode as reference. Measurements were performed in 0.5 mM CH₂Cl₂ solution, with tetrabutylammonium tetrafluoroborate as supporting electrolyte, at a scan rate of 50 mV/s. Each oxidation potential was calibrated using ferrocene as a reference.

Calculations. All (time-dependent) density functional theory (TD-DFT) calculations were carried out in the gas phase using the TURBOMOLE 5.10 quantum-chemical package, employing the B3LYP function and the 6-311G** basis set.³² TD-DFT was shown to reproduce the E* → K* ESIPT process until the biradical character began to dominate, which, in the gas phase, led to fast internal conversion via a conical intersection governed by torsional relaxation within the hydroxyphenyl imidazole unit.³³ Thus, TD-DFT sufficiently described the radiative processes of HPI and HPNI. To this end, vertical emission was calculated using a coplanar geometry of the K* form of the hydroxyphenyl imidazole backbone.

EL Device Fabrication. EL devices were fabricated with a configuration of (A) ITO/NPD (40 nm)/EML (W1, 30 nm)/BPhen (50 nm)/LiF (1 nm)/Al (100 nm) and (B) ITO/2-TNATA (60 nm)/NPD (20 nm)/EML (W1, 40 nm)/BPhen (20 nm)/LiF (1 nm)/Al (100 nm). All organic layers were deposited onto UV-O₃-treated indium–tin–oxide (ITO)-coated glass. All organic layers were deposited by thermal evaporation under a base pressure of <10^{−7} Torr. Deposition of a hole-transport layer of 600 Å (device B only; see Figure S10 in Supporting Information for details), a thick layer of 4,4',4''-tris(2-naphthylphenylamino)triphenylamine (2-TNATA), and a 400 or 200 Å thick layer of N,N'-diphenyl-N,N'-bis(1-naphthalenyl)-(1,1'-biphenyl)-4,4'-diamine (NPD) was followed by deposition of the emitting layer (W1). Over this layer, hole-blocking and electron-transport layers (500 or 200 Å of 4,7-diphenyl-1,10-phenanthroline [BPhen]) were sequentially deposited. Finally, 10 Å thick LiF and 1000 Å thick aluminum were successively deposited to form a cathode. The active area was 2 mm × 2 mm. Current–voltage–luminescence characteristics were obtained using a Keithley 237 source measurement unit and a Photoresearch PR-650 spectrometer.

Results and Discussion

The standard method for white-light generation typically involves mixing of the three primary colors red, green, and blue^{2,18–20} or combining two complementary colors.^{8,21} However, the simple mixing of luminescent materials can be problematic because color balancing is difficult to control as a result of near-inevitable energy transfer, leading to dominant emission from lower band-gap components, even when they are present in very small amounts.²² This energy transfer

(12) You, Y.; Kim, K. S.; Ahn, T. K.; Kim, D.; Park, S. Y. *J. Phys. Chem. C* **2007**, *111*, 4052.

(13) Kim, S.; Seo, J.; Jung, H. K.; Kim, J. J.; Park, S. Y. *Adv. Mater.* **2005**, *17*, 2077.

(14) (a) Klymchenko, A. S.; Pivovarenko, V. G.; Ozturk, T.; Demchenko, A. P. *New J. Chem.* **2003**, *27*, 1336. (b) Klymchenko, A. S.; Yushchenko, D. A.; Mely, Y. *J. Photochem. Photobiol. A* **2007**, *192*, 93.

(15) (a) Goodman, J.; Brus, L. E. *J. Am. Chem. Soc.* **1978**, *100*, 7472. (b) Kasha, M. *J. Chem. Soc., Faraday Trans. 2* **1986**, *82*, 2379.

(16) deMello, J. C.; Wittmann, H. F.; Friend, R. H. *Adv. Mater.* **1997**, *9*, 230.

(17) Berlman, I. B. *Handbook of Fluorescence Spectra of Aromatic Molecules*; Academic Press: New York, 1971.

(18) Gong, X.; Wang, S.; Moses, D.; Bazan, G. C.; Heeger, A. J. *Adv. Mater.* **2005**, *17*, 2053.

(19) (a) Aharon, E.; Kalina, M.; Frey, G. L. *J. Am. Chem. Soc.* **2006**, *128*, 15968. (b) Wu, C. C.; Sturm, J. C.; Register, R. A.; Thompson, M. E. *Appl. Phys. Lett.* **1996**, *69*, 3117.

(20) Kido, J.; Hongawa, K.; Okuyama, K.; Nagai, K. *Appl. Phys. Lett.* **1994**, *64*, 815.

(21) (a) Liu, J.; Guo, X.; Bu, L. J.; Xie, Z. Y.; Cheng, Y. X.; Geng, Y. H.; Wang, L. X.; Jing, X. B.; Wang, F. S. *Adv. Funct. Mater.* **2007**, *17*, 1917. (b) Qin, D. S.; Tao, Y. *Appl. Phys. Lett.* **2005**, *86*, 113507.

(22) (a) Van Der Meer, B. W.; Coker, G.; Chen, S. Y. S. *Resonance Energy Transfer: Theory and Data*; Wiley: New York, 1994. (b) Berggren, M.; Dodabalapur, A.; Slusher, R. E.; Bao, Z. *Nature* **1997**, *389*, 466.

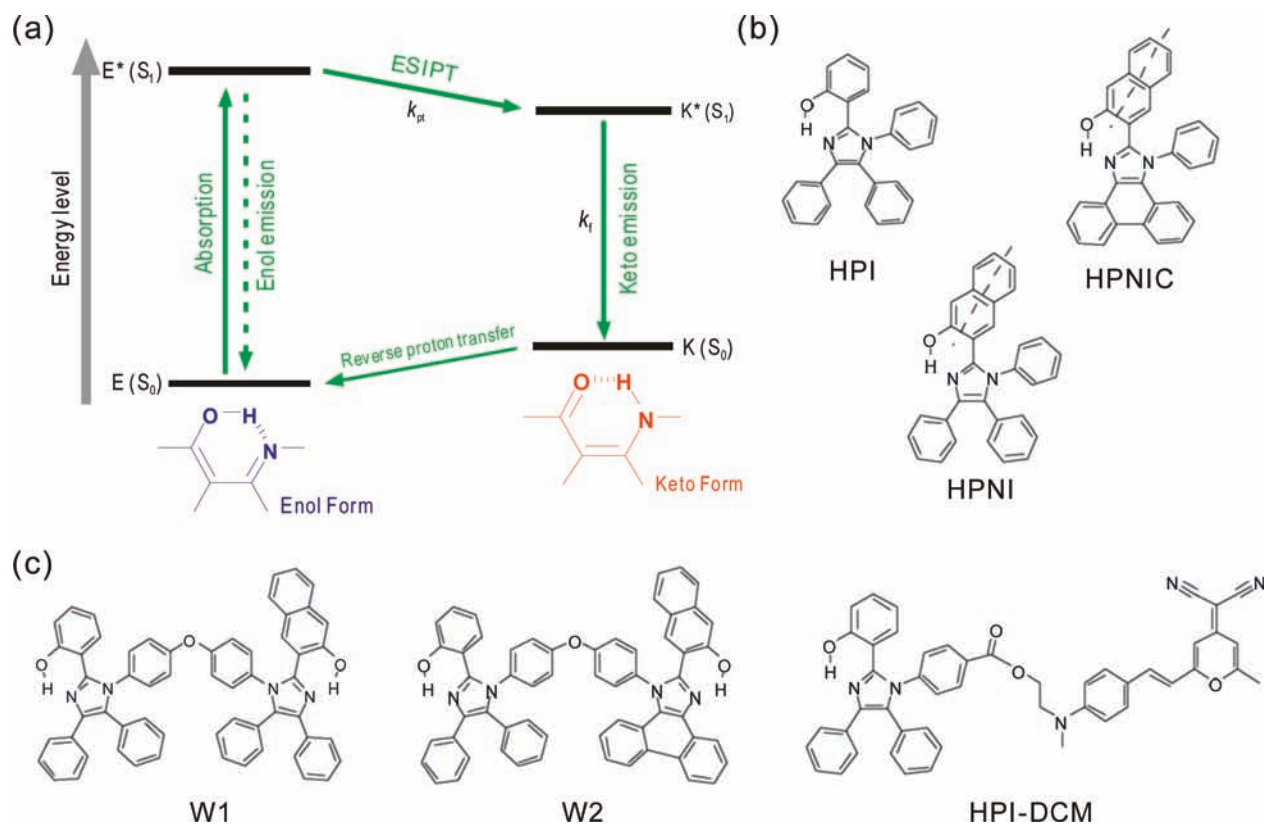


Figure 1. Schematic representation of the ESIPT photocycle and the structures of blue-, orange-, and white-light-emitting ESIPT molecules. (a) Characteristic four-level photocycle scheme of the ESIPT process. (b) Molecular structure of HPI, HPNI, and HPNIC. (c) Structures of white-light-emitting molecules based on ESIPT dyads. W1 and W2 were used to generate white light. The reference molecule HPI-DCM, which contains a conventional fluorophore, was also synthesized for comparative purposes.

originates from the interaction between an excited state donor with an acceptor in its electronic ground state. The extent of energy transfer depends on several parameters, including the radiative decay rate of the donor and the spectral overlap of donor emission and acceptor absorption, but especially on donor–acceptor separation and orientation, and thus critically on component concentration and the morphology of the final device. Therefore, complete frustration of energy transfer between donor and acceptor components is the only way to obtain stable color mixing in a single molecule; this has not been achieved to date.

To realize this aim, we designed a single molecular dyad composed of two ESIPT moieties in place of ordinary fluorescent materials. Each ESIPT moiety is characterized by a fast enol (E) to keto (K) cyclic intramolecular phototautomerization and demonstrates a high-energy UV enol absorption coupled with tunable keto emission.^{13,23–26} As summarized in Figure 1a, ESIPT-exhibiting molecules in the ground state exist exclusively as enol (E) forms, but upon photoexcitation, they undergo tautomerization into keto forms ($E^* \rightarrow K^*$) via an extremely fast and irreversible ESIPT process occurring in the

subpicosecond time domain.²⁷ After the excited keto form (K^*) decays radiatively to the intermediate ground state (K), the initial E form is instantaneously recovered. Therefore, predominant absorption from E and emission from K^* results in an anomalously large Stokes shift with no self-absorption, providing an ideal system for proton-transfer lasers^{27,28} and UV photostabilizers.²⁹ Moreover, it has been shown that proper molecular design and synthesis allowed the ESIPT keto emission wavelengths to be tuned over the whole range of the visible spectrum but with retention of enol form absorption in the UV region.³⁰ Therefore, the synthesis of a dyad composed of appropriate ESIPT fluorophores with complementary emission colors was expected to provide a novel and uncomplicated strategy for synthesis of a white-light-emitting single molecule by complete suppression of donor–acceptor energy transfer.

In the first step, because blue and orange are almost exactly complementary,²¹ we considered a combination of the blue-emitting ESIPT fluorophore 2-(1,4,5-triphenyl-1H-imidazol-2-yl)phenol (HPI, $\lambda_{\max} = 470$ nm, Figure 1b) and the orange-emitting fluorophore 2,5-bis(5-(4-*tert*-butylphenyl)-1,3,4-oxadiazol-2-yl)benzene-1,4-diol (DOX, used previously for demonstration

(23) Tarkka, R. M.; Zhang, X. J.; Jenekhe, S. A. *J. Am. Chem. Soc.* **1996**, *118*, 9438.

(24) Fischer, M.; Wan, P. *J. Am. Chem. Soc.* **1999**, *121*, 4555.

(25) (a) Park, S.; Kim, S.; Seo, J.; Park, S. Y. *Macromolecules* **2005**, *38*, 4557. (b) Park, S.; Seo, J.; Kim, S. H.; Park, S. Y. *Adv. Funct. Mater.* **2008**, *18*, 726. (c) Park, S.; Kim, S.; Seo, J.; Park, S. Y. *Macromol. Res.* **2008**, *16*, 385. (d) Park, S.; Kwon, O. H.; Lee, Y. S.; Jang, D. J.; Park, S. Y. *J. Phys. Chem. A* **2007**, *111*, 9649.

(26) Klymchenko, A. S.; Demchenko, A. P. *J. Am. Chem. Soc.* **2002**, *124*, 12372.

(27) Khan, A. U.; Kasha, M. *Proc. Natl. Acad. Sci. U.S.A.* **1983**, *80*, 1767.

(28) Chou, P.; Mcmorrow, D.; Aartsma, T. J.; Kasha, M. *J. Phys. Chem.* **1984**, *88*, 4596.

(29) Goeller, G.; Rieker, J.; Maier, A.; Stezowski, J. J.; Daltrozzi, E.; Neureiter, M.; Port, H.; Wiechmann, M.; Kramer, H. E. A. *J. Phys. Chem.* **1988**, *92*, 1452.

(30) (a) Chen, K. Y.; Hsieh, C. C.; Cheng, Y. M.; Lai, C. H.; Chou, P. T. *Chem. Commun.* **2006**, 4395. (b) Chou, P. T.; Huang, C. H.; Pu, S. C.; Cheng, Y. M.; Liu, Y. H.; Wang, Y.; Chen, C. T. *J. Phys. Chem. A* **2004**, *108*, 6452. (c) Seo, J.; Kim, S.; Park, S.; Park, S. Y. *Bull. Korean Chem. Soc.* **2005**, *26*, 1706.

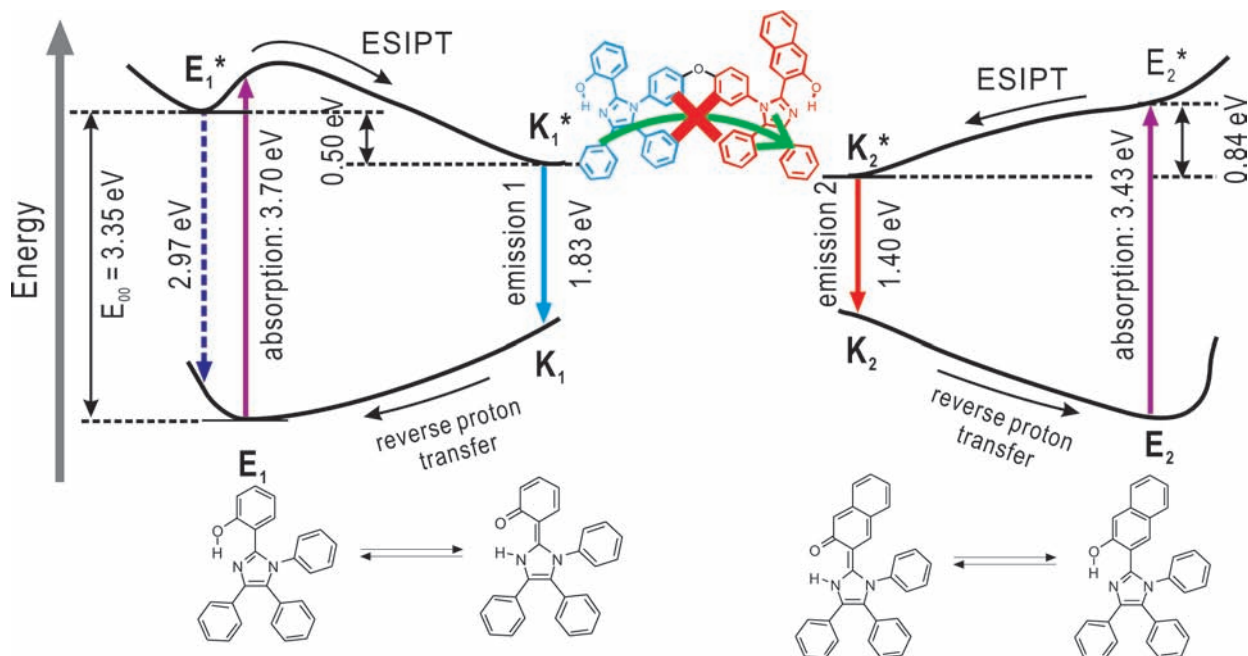


Figure 2. Diagram of the ES IPT process in the white-light-emitting molecular dyad. Calculated energy level in W1, with the HPI moiety on the left and HPNI on the right, according to TD-DFT calculations.

of frustrated energy transfer; $\lambda_{\max} = 580$ nm; see Scheme S4 in Supporting Information (SI) as constituent emitting centers for white-light emission.^{13,31} However, it appeared that the rigid molecular structure of DOX made it insoluble in common organic solvents and thus made the synthesis and handling of DOX fragments difficult. Fortunately, a simpler alternative orange keto-emitting ES IPT unit was successfully synthesized by replacing the phenyl group of HPI by the naphthalene group [3-(1,4,5-triphenyl-1*H*-imidazol-2-yl)naphthalen-2-ol (HPNI) of Figure 1b]. In the newly synthesized HPNI molecule, the naphthalene group significantly stabilized the energy of the excited-state keto form by enhancement of conjugation via delocalization of π electrons along the naphthalene backbone (the dashed line on the HPNI structure).³² Consequently, HPNI showed a huge bathochromic shift of photoluminescence (PL) compared to HPI ($\lambda_{\max} = 570$ vs 470 nm). The emission was tuned even more to the red ($\lambda_{\max} = 590$ nm) by linking the 4,5-phenyl rings of HPNI to synthesize 3-(1-phenyl-1*H*-phenanthro[9,10-*d*]imidazol-2-yl)naphthalen-2-ol (HPNIC, Figure 1b). Finally, by covalently linking molecular pairs, the dyad molecules W1 and W2 were synthesized (Figure 1c).

In the design of W1 and W2 molecular dyads, an ether linkage between the fluorophores was chosen because diphenylether is a simple but chemically very stable cross-linking group.³³ Quantum-chemical calculations on W1 and W2 using density functional theory (DFT B3LYP/6-311G**, see SI for details) indicated an almost perpendicular molecular conformation of the phenyl rings within the diphenylether unit (Figures S1–S3 in SI). This further reduces the electronic communication between the ES IPT moieties and limits intermolecular stacking in the solid state.^{34,35}

Although the synthetic route to the W1 and W2 dyads (see Schemes S1 and S2 in SI) comprised only two initial steps, the reaction scheme was later adjusted to include four steps for convenience of purification of the crude product (compare Schemes S1 and S3 in SI). Briefly, the HPI derivative with an acetamide side group was synthesized by refluxing salicylaldehyde, benzil, 4,4'-oxidianiline, and ammonium acetate in acetic acid. Next, the acetamide group was deblocked by hydrochloric acid to give the free amine. To synthesize the HPNI and HPNIC materials, 2-hydroxy-3-naphthaldehyde was prepared by direct formylation of 2-naphthol using *tert*-butyllithium at room temperature. Finally, W1 and W2 were obtained with high yields of 65 and 60%, respectively. Note that easy synthesis of the W1 and W2 dyads are essential for real applications in optoelectronic and lighting devices.

Figure 3a shows the UV/vis absorption and PL spectra of the individual chromophores HPI, HPNI, and HPNIC in solution (CHCl_3 , $c = 1 \times 10^{-5}$ M). Common electronic absorption by HPI and HPNI was found in the region 320–350 nm, where both species can be simultaneously photoexcited. Low-energy absorption features correspond to singlet π - π^* excitation of the enol ground state (E) to the first excited state, $E \rightarrow E^*$ ($S_0 \rightarrow S_1$), consistent with the time-dependent (TD)-DFT calculations, as shown in Figure 2; for details see SI. After photoexcitation ($E \rightarrow E^*$), intramolecular proton transfer (ES IPT) generates the keto excited state (K^*), calculated to be lower in energy than E^* by 0.5 and 0.84 eV for HPI and HPNI, respectively. Next, intense keto PL with maxima at 470 nm (HPI), 570 nm (HPNI), and 590 nm (HPNIC) were observed (see Table 1). The large Stokes' shifts of about 8600, 9500, and 10 100 cm^{-1} , respectively, confirmed that emission arose

(31) Park, S.; Kwon, O. H.; Kim, S.; Park, S.; Choi, M. G.; Cha, M.; Park, S. Y.; Jang, D. *J. Am. Chem. Soc.* **2005**, *127*, 10070.

(32) Nagaoka, S.; Nakamura, A.; Nagashima, U. *J. Photochem. Photobiol. A* **2002**, *154*, 23.

(33) Ma, H.; Chen, B. Q.; Sassa, T.; Dalton, L. R.; Jen, A. K. Y. *J. Am. Chem. Soc.* **2001**, *123*, 986.

(34) Ahlrichs, R.; Bar, M.; Haser, M.; Horn, H.; Kolmel, C. *Chem. Phys. Lett.* **1989**, *162*, 165.

(35) (a) Wu, Y. G.; Lawson, P. V.; Henary, M. M.; Schmidt, K.; Bredas, J. L.; Farni, C. *J. Phys. Chem. A* **2007**, *111*, 4584. (b) Barbatti, M.; Aquino, A. J. A.; Lischka, H.; Schriever, C.; Lochbrunner, S.; Riedle, E. *Phys. Chem. Chem. Phys.* **2009**, *11*, 1406.

Table 1. Optical and Photophysical Properties of the Compounds under Study: Absorption and PL Maxima ($\lambda_{\text{max,abs}}$, $\lambda_{\text{max,em}}$), Molar Extinction Coefficients (ϵ), PL Quantum Yields, and Decay Times (Φ_{PL} , τ_{PL})

	$\lambda_{\text{max,abs}}$, nm	ϵ^a L mol ⁻¹ cm ⁻¹	$\lambda_{\text{max,em}}$, nm	Φ_{PL}^b	τ_{PL} (ns) at λ (nm)
HPI	320	0.42×10^4	470	0.35	2.0 (450)
HPNI	331	1.14×10^4	570	0.22	5.9 (580)
HPNIC	337	1.14×10^4	590	0.16	3.8 (580)
W1	HPI: 320 HPNI: 332	1.59×10^4	HPI: 472 HPNI: 564	0.27	2.5 (450) 6.5 (680)
W2	HPI: 320 HPNIC: 333	1.59×10^4	HPI: 473 HPNIC: 586	0.22	3.4 (450) 2.7 (580)

^a HPI, HPNI, W1 (346 nm); HPNIC, W2 (345 nm). ^b The PL quantum yields (Φ_{PL}) of HPI, HPNI, HPNIC, W1, and W2 were measured using an integrating sphere and an emission-tunable CW He–Cd laser.^{16,17}

from $\text{K}^* \rightarrow \text{K}$ transitions, whereas $\text{E}^* \rightarrow \text{E}$ emission was seen as only very weak shoulders.^{13,25} After reaching the keto ground state (K), the enol form (E) was instantaneously recovered, with the latter being about 1.0 eV lower than K with no transient energy barrier; see Figure 2. The excitation spectra, monitored at the respective emission bands, were spectrally identical to the lowest absorption band, indicating that both PL bands originated from the same initially excited species. We wish to stress that absorptions of the orange-emitting HPNI and HPNIC molecules are located in the UV region and show no significant spectral overlaps with HPI emission. The other noteworthy feature of HPNI is that the ground state of actual emitter (K_2) is only transient and thus statistically unpopulated. Therefore, in a 1:1 mixture of donor (D = HPI) and acceptor (A = HPNI, HPNIC), energy transfer (which is proportional to the D–A electronic interaction including spectral overlap)³⁶ is virtually blocked, unlike in common D–A systems containing ordinary blue- and orange-emitting molecules.

On the basis of this theoretical background, we expected to see broad white-light emission after 1:1 blending or covalent tethering of the blue- and orange-light-emitting components. Indeed, in the synthesized molecular dyads W1 and W2, the full spectrum of visible light was covered by the two simultaneously occurring emissions (Figure 3b,c). Because energy transfer is completely blocked between the emitting centers, the dyad emissions are simply the superposition of those from the individual centers, as shown in Figure 3b,c for W1 and W2, respectively.

The actual emission color of the dyad is quite sensitive to and precisely controllable by the excitation wavelength because the extinction coefficients of HPI and HPNI (HPNIC) are not identical within their entire absorption ranges. This is an interesting phenomenon since precise color-tuned emission from a single molecule using varying excitation wavelengths is very uncommon. In particular, as depicted in Figure 3, W1 and W2 could be tuned to exhibit pure white emission by 346 and 345 nm excitation, respectively (see photographs in Figure 4a), where blue- and orange-light emission intensities were well equilibrated. For W1, the molar absorption coefficients (ϵ values) of HPI and HPNI at 346 nm were 4.2×10^3 and 1.14×10^4 M⁻¹ cm⁻¹, respectively, but the emission intensity ratio between HPI and HPNI in Figure 3b was less pronounced because of the higher PL quantum yield of HPI compared to HPNI (Table 1). At 320 nm excitation, however, W1 showed a blue-dominant

broad emission because of an increase in HPI absorption ($\epsilon = 1.77 \times 10^4$ M⁻¹ cm⁻¹), and emission was thus comparable to that of HPNI ($\epsilon = 1.71 \times 10^4$ M⁻¹ cm⁻¹). Similarly, at 350 nm excitation wavelength, the emission became more orange because of the lower absorption of HPI compared to that of HPNI (details are given in Figure S6 in SI).

The actual emission spectrum of W1 or W2 can be simply approximated by a sum of emissions from the individual components from the ratio of their extinction coefficients and emission intensities obtained under these conditions, as seen by comparison of the green solid and dashed lines in Figure 3b,c. Note that the summation procedure is applicable at any other excitation wavelength, as shown in Figure S6 in SI, yielding unambiguous evidence for frustrated energy transfer between the emitting components of the dyad structure. On the basis of the same reasoning, the quantum yield Φ_{PL} of the dyad was estimated from those of its components (c_1, c_2) as follows:

$$\Phi_{\text{PL}}(c_1 + c_2) = \{\Phi_{\text{PL}}(c_1)\epsilon(c_1) + \Phi_{\text{PL}}(c_2)\epsilon(c_2)\} / \epsilon(c_1 + c_2) \quad (1)$$

For W1, with $c_1 = \text{HPI}$ and $c_2 = \text{HPNI}$, the quantum yield was estimated to be $\Phi_{\text{PL}}(\text{HPI} + \text{HPNI}) = 0.28$, quite close to the measured value of $\Phi_{\text{PL}}(\text{W1}) = 0.27$ (see Table 1). In our study, the fluorescence quantum yields of the W1 molecule as well as its emission spectrum were found to be virtually invariant with the environmental changes including the solvent polarity and the added protic solvent (see Figure S13 in SI), unlike the conventional ESIPT materials. This is uniquely attributed to the strong and planar intramolecular H bond in HPI enclosed with bulkier steric groups like 1- and 5-phenyl substituents.

For comparison, we investigated HPI–DCM (Figure 1c), containing a classical (non-ESIPT) fluorophore. This compound showed almost completely red-shifted orange emission with only a small shoulder in the blue HPI region, and simple summation of components was obviously inapplicable (see Figure 3d). This might be attributed to efficient energy transfer from HPI to the DCM fragment because of the great spectral overlap between the HPI emission and the DCM absorption at around 470 nm (Figure 3d and Figure S8 in SI). This observation emphasizes the beneficial features of frustrated energy transfer in the W1 and W2 dyads.

Further evidence for frustrated energy transfer was derived from fluorescence lifetime measurements.^{35,37} Unlike conventional observations on resonant energy transfer, where the presence of acceptor molecules leads to shorter fluorescence donor decay times ($\tau_{\text{PL,D}}$ values), the donor unit (HPI) lifetimes in W1 with $\tau_{\text{PL,D}} = 2.5$ ns and in W2 with $\tau_{\text{PL,D}} = 3.4$ ns were comparable to or even slightly greater than that of HPI (2.0 ns); see Table 1 and Figure S10 in SI for details. Because of the total frustration of energy transfer, the white-light emissions from W1 and W2 were also completely independent of concentration or state. When we measured PL spectra at different concentrations, the peak-normalized spectra of all samples were identical (Figure 4c). Furthermore, white-light emission was observed not only in solution but also in the solid state (thin films of dyes dispersed in poly(methylmethacrylate), PMMA; see Figure 4a). In addition to the frustrated energy transfer between D–A units, it is considered that both twisted ether linkages and bulky aromatic rings in the HPI and HPNI units assist in preventing direct stacking of active chromophores, thereby maintaining appropriate intermolecular distances and suppressing concentration-dependent PL quenching, and thus permitting strong emission.³¹

(36) Turro, N. J. *Modern Molecular Photochemistry*; University Science Books: Sausalito, CA, 1991; Chapter 9.

(37) Jarvis, G. B.; Mathew, S.; Kenny, J. E. *Appl. Opt.* **1994**, *33*, 4938.

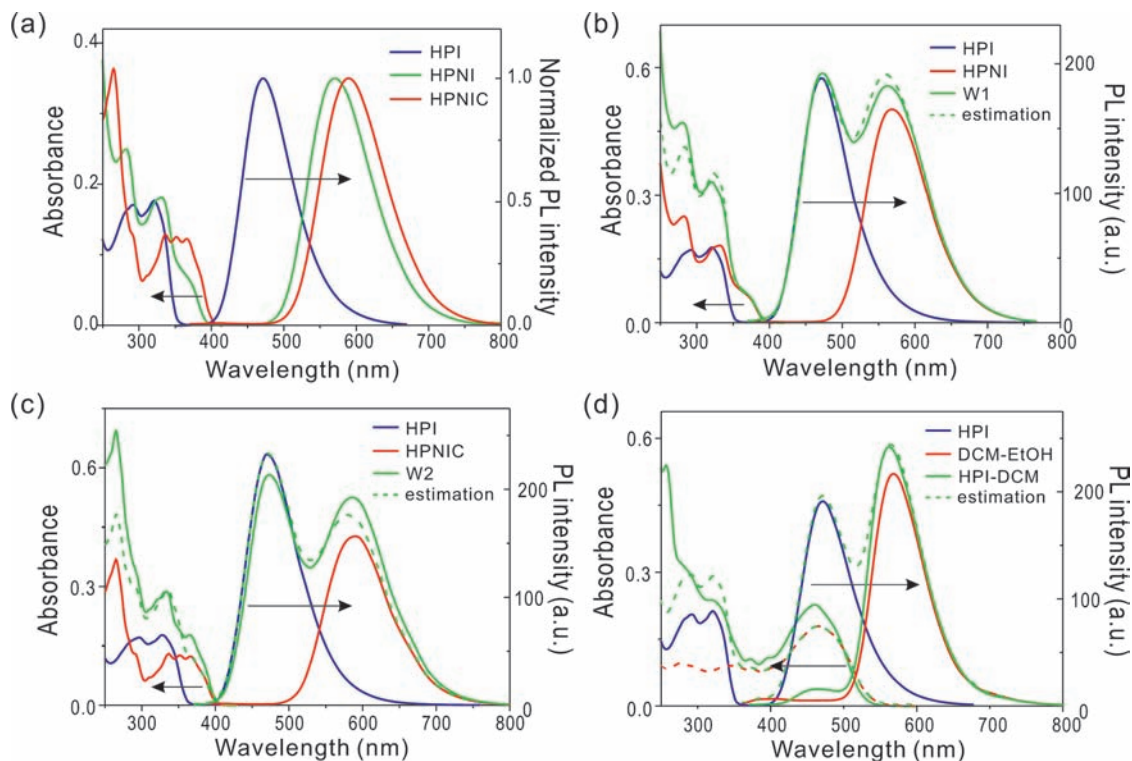


Figure 3. Optical properties of synthesized molecules in solution (CHCl_3 , $c = 1 \times 10^{-5}$ M) at room temperature. (a) Absorption (Abs) and normalized photoluminescence (PL) of HPI (blue), HPNI (green), and HPNIC (red). (b) Abs and PL (excitation at 346 nm) spectra of HPI (blue), HPNI (red), and W1 (green solid line). The green dashed line indicates the expected spectrum of W1 as a superposition of HPI and HPNI (see text). (c) Abs and PL (excitation at 345 nm) spectra of HPI (blue), HPNIC (red), and W2 (green solid line). The green dashed line indicates the expected spectrum of W2 as a superposition of HPI and HPNIC. (d) Abs and PL (excitation at 345 nm) spectra of HPI (blue), DCM-EtOH (red), HPI-DCM (green solid line), and the expectation (green dashed line).

Finally, the proposed PL additivity from complementary emitting centers was verified by examination of CIE coordinates (x, y) of compound emission colors. Initial CIE coordinates of HPI (0.16, 0.23), HPNI (0.49, 0.50), and HPNIC (0.52, 0.47) clearly lay on a straight line (see dashed line in Figure 4b), passing through the ideal white values (0.33, 0.33), thus constituting complementary colors. It is noteworthy that the CIE coordinates of both solutions and films were similar. The slight differences may be attributed to the higher polarizability of the surrounding medium in the solid state.^{38,39}

To synthesize single-molecule-based white-light-emitting organic light-emitting devices, using W1 as the emission layer, two simple electroluminescence (EL) devices were fabricated with a configuration of (A) ITO/2-TNATA(60 nm)/NPD (20 nm)/EML(W1, 40 nm)/BPhen(20 nm)/LiF(1 nm)/Al(100 nm) and (B) ITO/NPD(40 nm)/EML(W1, 30 nm)/BPhen(50 nm)/LiF(1 nm)/Al(100 nm), with and without insertion of a hole injection layer, respectively (see Figures S11 and S12 and Table S1 in SI for details). The W1 electroluminescence (EL) spectra from either A or B appeared very similar to the PL spectra, with blue and orange emission bands, generated from the HPI and HPNI moieties, respectively (Figure 4d). The development of EL is attributable to the presence of an electrically initiated ESIPT in each constituent emitting center (HPI/HPNI); the exciton is formed by recombination of an electrically generated hole E^+ and an electron E^- within the emitting layer, yielding E^* , which then decays via K^* , as in PL.^{13,23} However, a

significant dependency of HPI and HPNI emission intensity ratios on the device structure was observed (Figure 4d), which can be rationalized by DFT calculations. Of the potential electron-transporting species (HPI^- , HPNI^-) it was calculated that HPNI^- is preferentially formed because of the much higher electron affinity (EA) compared to HPI (Table S3 in SI). However, the ionization potentials of both HPI and HPNI are of the same order, suggesting that formation of both HPI^+ and HPNI^+ might sensitively depend on the local environment. Considering that these cationic species are responsible for primary exciton formation in geminate recombination, a sensitive dependency of emission characteristics on device morphology, particularly the presence or absence of a hole injection layer, was both expected and observed. Much like the excitation wavelength control on the emission color (vide supra), the injection and transport control by the device structure in EL is rationalized to work similarly.

In contrast to the behavior of the more blue-side emitting device A, device B, without the 2-TNATA layer, yielded time- and bias-stable white-light EL with CIE (x, y) coordinates of (0.34, 0.29); see Figure 4b. The stable EL spectra were probably attributed to the high T_g of W1 (~ 143 °C) and W2 (~ 153 °C) molecules, which prevents any morphological changes of the emission layer under device operation. The turn-on voltage was 6.7 V, and the maximum luminous efficiency was 0.98 cd/A, corresponding to an external quantum efficiency of 0.76%. The maximum brightness of the device was 1092 cd/m^2 (see Figures S11 and S12 and Table S2 in SI for details). Although EL device performance has not yet been optimized, it is encouraging that a single-molecule-based white-light-emitting OLED has been

(38) Gierschner, J.; Cornil, J.; Egelhaaf, H. J. *Adv. Mater.* **2007**, *19*, 173.

(39) Cornil, J.; Beljonne, D.; Calbert, J. P.; Bredas, J. L. *Adv. Mater.* **2001**, *13*, 1053.

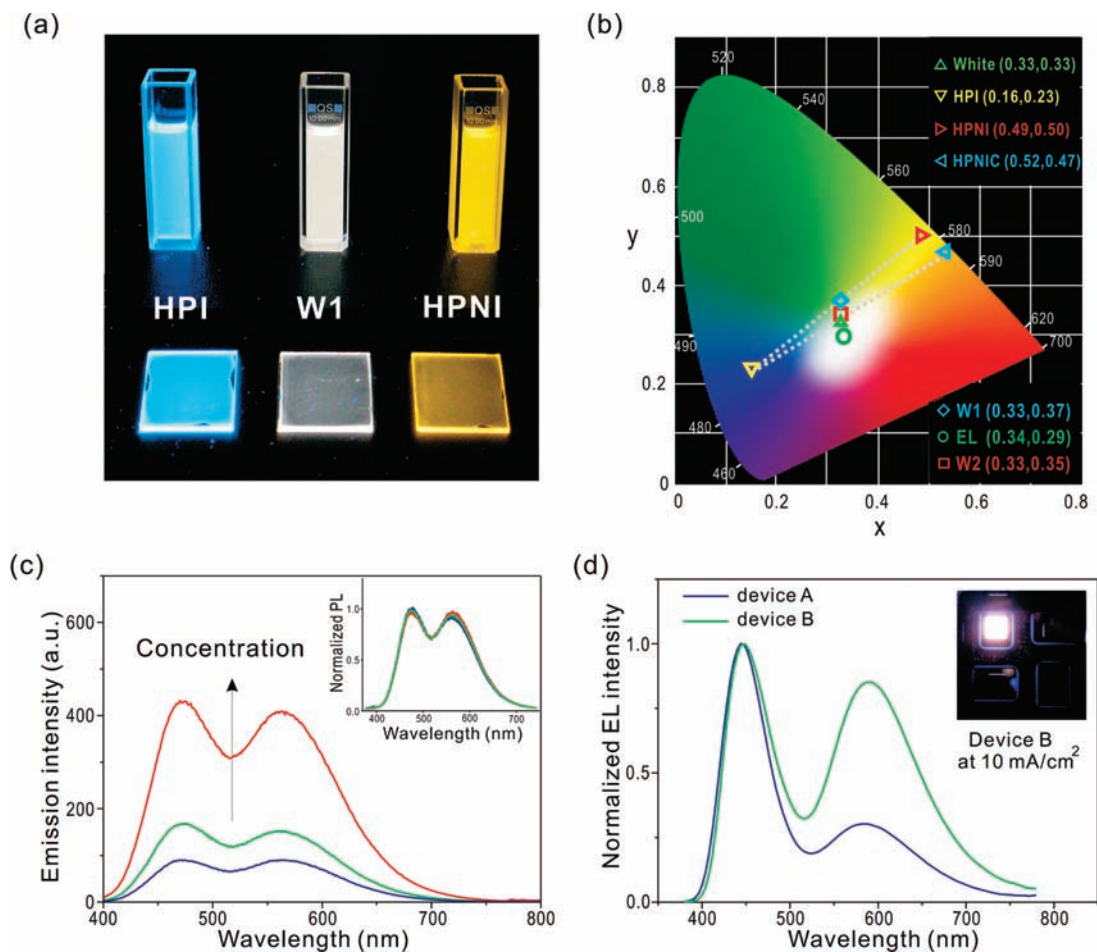


Figure 4. Photo- and electroluminescence from the white-light-emitting molecular dyads. (a) Photographs of HPI, W1, and HPNI molecules in solution (1×10^{-5} M in CHCl_3) and thin films of the compounds on PMMA ($c = 1$ wt %) under UV light (365 nm hand-held UV lamp, $1.2 \text{ mW} \cdot \text{cm}^{-2}$). (b) Emission colors in a CIE 1931 chromaticity diagram: Ideal white (Δ , 0.33, 0.33); HPI (∇ , 0.16, 0.23); HPNI (\triangleright , 0.49, 0.50); HPNIC (\triangleleft , 0.52, 0.47); PL of W1 (\diamond , 0.33, 0.37); EL of W1 (\circ , 0.34, 0.29); EL of W2 (\square , 0.33, 0.35). (c) PL spectra of W1 at different concentrations (1×10^{-3} to 1×10^{-5} M in CHCl_3). The excitation wavelength was 346 nm. The inset shows the normalized spectra of each sample. (d) EL spectra of device A (blue) and device B (green) at 10 mA/cm^2 . The inset shows the operation image of device B at 10 mA/cm^2 .

fabricated. Finally, it should be mentioned that our HPI, HPNI, and HPNIC moieties showed excellent photostability upon UV irradiation. Even when molecules were repeatedly exposed to 355 nm picosecond Nd:YAG laser pulses ($\sim 5 \times 10^5$ shots), no discernible photobleaching or decomposition was observed using an excitation power of $2 \text{ mJ cm}^{-1} \text{ pulse}^{-1}$.

In conclusion, an ideal material for a white-light source should be cost-effective, stable, robust, emit over the whole visible spectrum, not suffer from self-absorption, and its pure color should be easily reproducible.⁴⁰ With this goal in mind, we have successfully synthesized and characterized, for the first time, a white-light-emitting single molecule dyad, consisting of two noninteracting chromophores showing excited-state intramolecular proton transfer (ESIPT). This unprecedented example of a concentration-independent ultimate white-light-emitting molecule not only blocks energy transfer between a wide band-gap donor and a smaller band-gap acceptor but also shows reproducible and stable white photo- and electroluminescence. The molecule is expected to have a significant impact on the development of a new class of displays and light sources.

(40) Bowers, M. J.; McBride, J. R.; Rosenthal, S. J. *J. Am. Chem. Soc.* **2005**, *127*, 15378.

Acknowledgment. This work was supported by the Korea Science and Engineering Foundation (KOSEF) through the National Research Laboratory Program (2006-03246) and Creative Research Initiatives Program (0417-20090011) funded by the Ministry of Education, Science of the Korea Government. We are grateful for the instrumental and partial financial support of Dongwoo FineChem Co., Ltd. D.-J.J. and S.-Y.P. thank the SRC program (R11-2007-012-01002-0) and the BK 21 Program, respectively. B.M.M. thanks the Ministerio de Ciencia e Innovación of Spain (MCI) for a “Juan de la Cierva” contract. J.G. is a “Ramón y Cajal” Research Fellow, financed by the MCI; at present he is a visiting researcher at the ICMol, Valencia, under the auspices of the Consolider Ingenio 2010 Nanoscience program. J.G. and B.M.M. thank P. Viruela for helpful discussions.

Note Added after ASAP Publication. The version published on May 29, 2009 contained an error in equation 1. The corrected version was published July 13, 2009.

Supporting Information Available: Synthesis, measurements, calculation, and EL device fabrication details are given. This material is available free of charge via the Internet at <http://pubs.acs.org>.

JA902533F